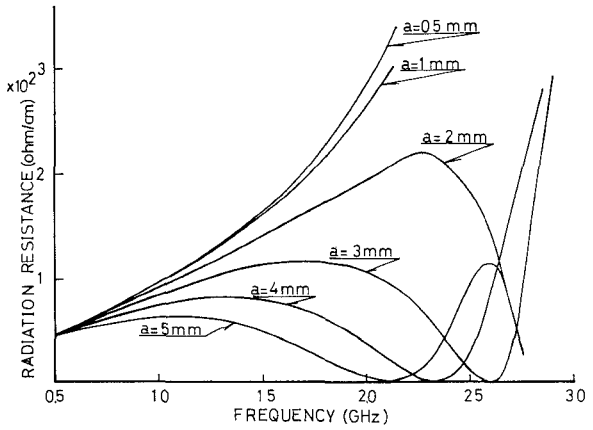

Fig. 2. Radiation resistance is plotted as a function of frequency for the radius of the inner conductor $a = 0.2$, 0.5, 1.0, 2.0, 3.0, and 4.0 m/m. Other parameters are biasing dc magnetic field $h = 500$ oe, saturation magnetization $4\pi M_s = 1800$ g.

condition is

$$e_z = a_0\left(J_0(k\sigma) - \frac{J_0(ka)}{H_0^{(2)}(ka)} H_0^{(2)}(k\sigma)\right). \tag{9}$$

As shown in Fig. 1, an infinitely long wire is situated parallel to the z axis, so the current flowing into the wire excites the RF magnetic fields h_θ. This means that the power flowing into the wire (RF current j_s) is equal to the radiating power. Since the energy dissipation is zero in the region of the field bounded by a surface S, the real part of complex Poynting vector is zero

$$\mathrm{Re}\left(\frac{1}{2}\int_S (-e_z h_\theta^*)\,\sigma\, d\theta\right) = 0 \tag{10}$$

where h_θ^* is the complex conjugate of h_θ. From Maxwell's equation, we have a relation between e_z and h_θ

$$h_\theta = \left(\frac{-\mu}{\mu^2 - \kappa^2}\right)\left(\frac{1}{j\omega\mu_0}\right)\frac{\partial^e z}{\partial \sigma}. \tag{11}$$

According to Ampere's law, we have a relation between the current j_s and the amplitude a_0 of (6)

$$j_s = \int_0^{2\pi} h_\theta a\, d\theta. \tag{12}$$

This relation gives

$$a_0 = \frac{-j_s}{2\pi a}\frac{(\mu^2 - \kappa^2)\, j\omega\mu_0}{\mu k}\left(J_1(ka) - \frac{J_0(ka)}{H_0^{(2)}(ka)} H_1^{(2)}(ka)\right)^{-1} \tag{13}$$

The radiation resistance R_m is defined by the ratio the radiative power to the square of the current flowing into the metal cylinder

$$R_m = \frac{1}{16}\frac{\omega\mu_0}{k}\frac{\mu^2 - \kappa^2}{\mu}(J_0(ka))^2. \tag{14}$$

In Fig. 2, the radiation resistance R_m is plotted as a function of frequency. The important characteristics (shown in Fig. 2) are that this device transmits all signals from direct current up to some frequency near the critical frequency $\omega = \gamma(BH)^{1/2}$. This extremely wide bandwidth can be achieved by reducing the radius of the metallic wire a. Note that for $a = 0.5$ m/m, 1 to 2 thousand megahertz excitation bandwidths are possible. Owing to the above reasons, development of a suitable radial line should produce extremely wide bandwidths and magnetically tunable low frequency (0.5 to 1 GHz) microwave transducer.

References

[1] A. K. Ganguly and D. C. Webb, *IEEE Microwave Theory Tech.*, vol. MTT-23, p. 998, 1975.
[2] J. C. Sethares, *IEEE Microwave Theory Tech.*, vol. MTT-27, p. 902, 1979.
[3] P. R. Emtage, *J. Appl. Phys*, vol. 49, p. 4475, 1978.
[4] C. Vittoria and N. D. Wilsey, *J. Appl. Phys.*, vol. 45, p. 414, 1974.
[5] Y. S. Wu and F. J. Rosenbaum, *J. Appl. Phys.*, vol. 45, p. 2512, 1974.
[6] M. L. Kales, *J. Appl. Phys.*, vol. 24, p. 604, 1953.
[7] A. G. Gurevich, *Ferrites at Microwave Frequencies* Boston, MA: Boston Tech Pub., 1965. Massachusetts, 1965.

Broad-Band Design of Improved Hybrid-Ring 3-dB Directional Couplers

DONG IL KIM, STUDENT MEMBER, IEEE, AND YOSHIYUKI NAITO, SENIOR MEMBER, IEEE

Abstract—**A broad-band design theory of an improved 3-dB hybrid-ring directional coupler is proposed and discussed. The synthesis of the improved broad-band hybrid-ring directional coupler starts by applying the concept of hypothetical port and generalizing the conventional hybrid-ring. The improved broad-band 3-dB hybrid-rings can be constructed very easily and their bandwidths are considerably wide, while the bandwidth of the reverse-phase hybrid-ring (one lambda ring) may be increased to approximately an octave, but it has not found wide acceptance because of its extreme difficulty of construction. The bandwidth of the improved broad-band 3-dB hybrid-ring directional coupler is 1.84 times as wide as the conventional rat race or hybrid-ring, extending from 0.747 to 1.253 in normalized frequency. Furthermore, the experimental verification has been achieved in microstrip network, and, hence, the validity of the design method proposed in this paper is confirmed. Although only the 3-dB hybrid-ring directional was considered here, the method itself is to be applicable to a hybrid-ring directional coupler with any degree of coupling.**

I. Introduction

A hybrid-ring directional coupler is one of the fundamental components used in microwave circuits, which is recognized as a rat race ring when it is used for a 3-dB directional coupler with the normalized admittance of $1/\sqrt{2}$ on the whole circumference on the ring. The rat race or hybrid-ring directional coupler has the bandwidth of approximately 27.6 percent at the tolerance limits of the deviation of 0.43 dB for split and of 20 dB for the maximum return loss and isolation.

This paper describes two methods for broadening the bandwidth of the hybrid-ring while it operates as a 3-dB directional coupler. The broad-band design method proposed here was accomplished using CAD, in which the concept of hypothetical

Manuscript received January 22, 1982; revised April 28, 1982. This work was supported in part by the Ministry of Education, Japan, under Contract 56460108.

The authors are with the Department of Electrical and Electronic Engineering, Tokyo Institute of Technology, Meguro-ku, Tokyo 152, Japan

0018-9480/82/1100-2040$00.75 ©1982 IEEE

port and Powell's minimizing method were used. The bandwidth of the 3-dB hybrid-ring directional coupler has been increased by 50.7 percent. The frequency characteristics of the improved hybrid-ring are compared with those of the conventional rat race and hybrid-ring. The bandwidth was broadened tremendously by dividing the three-quarter-wave equal-admittance section on the ring of the conventional hybrid-ring as a result of adopting the concept of hypothetical port, and by adding quarter-wave transformers to the original port.

II. Approach to the Broad-band Design

In general, the 4-port hybrid-ring directional coupler shown in Fig. 1(a) can be regarded as a 6-port one with 2 hypothetical ports of $h5$ and $h6$ as shown in Fig. 1(b), while these hypothetical ports are terminated with open-circuits in the case of the conventional 4-port. The way of thinking like this is very effective in certain cases. For example, a lossless power divider with 3 ports with no reflection at each port cannot be realized, but a 2-way power divider with 4 ports can be done even though one of the 4 ports is terminated with a proper absorbing resistance. Hence, in this case, the terminated port might be regarded as a hypothetical port. Another example is that a broad-band circulator [1] is obtained by loading properly the compensating circuits at the hypothetical ports after establishing 3 hypothetical ports among the three original ports.

We can generalize the conventional hybrid-ring directional coupler as shown in Fig. 1(b) by establishing two hypothetical ports $h5$ and $h6$, and by replacing the characteristic admittance Y_1 on the three-quarter-wave section of the conventional or original hybrid-ring with Y_3 of two quarter-wave sections and Y_4 of one-quarter-wave section. Here, we assume that the compensating circuits for the hypothetical ports are as shown in Fig. 2. Then, the input admittance for the compensating circuits Y_s is given by

$$Y_s = Y_{s1}\frac{j\{Y_{s1}\tan\beta l_{s1} + Y_{s2}\tan\beta l_{s2}\}}{Y_{s1} - Y_{s2}\tan\beta l_{s1}\tan\beta l_{s2}} \tag{1}$$

where $\beta l_{s1} = (2\pi/\lambda_g)l_{s1} = 8\theta l_{s1}/\lambda_0$, $\beta l_{s2} = 8\theta l_{s2}/\lambda_0$, $\theta = \pi/4(f/f_0)$, f and f_0 are the operating frequency and the design center frequency, Y_{s1} and Y_{s2} are the characteristic admittances, and l_{s1} and l_{s2} are the lengths of the compensating stubs, respectively. The scattering matrix of the assumed circuit as shown in Fig. 2 is obtained in the same manner as for the conventional hybrid-ring [2], [3]

$$[S] = \begin{pmatrix} S_{11} & S_{12} & S_{13} & S_{14} \\ S_{12} & S_{22} & S_{23} & S_{13} \\ S_{13} & S_{23} & S_{22} & S_{12} \\ S_{14} & S_{13} & S_{12} & S_{11} \end{pmatrix} \tag{2}$$

where $S_{ij} = S_{ij}(Y_1, Y_2, Y_3, Y_4, Y_{s1}, Y_{s2}, l_{s1}, l_{s2})$.

It is generally required in the actual characteristics of a directional coupler or a power divider that the couplings, matching, and isolation are to be within certain tolerance limits over a broad frequency band even though the circuit may not be perfectly matched and isolated at the center frequency. Although the tolerance limits for couplings, matching, and isolation depend upon the degree of performance required, e.g., ± 0.5 dB for coupling deviations and 20 dB for maximum reflection and isolation in the case of a balanced amplifier, throughout this paper we take the tolerance limits of ± 0.43 dB for the coupling deviations and 20 dB for maximum reflection and isolation. Considering the required characteristics of the 3-dB directional coupler included broadbanding, we define an evaluation function

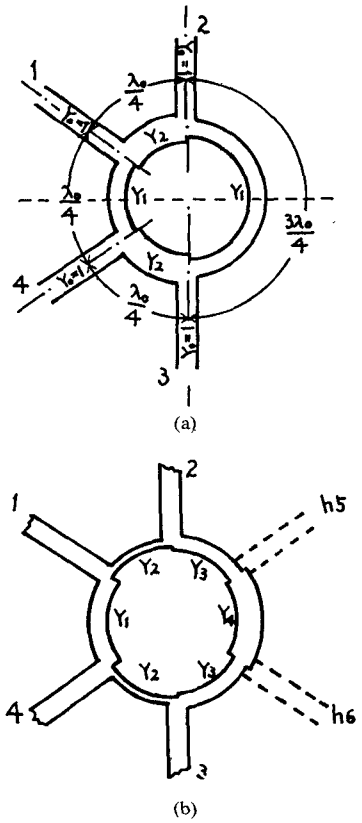

Fig. 1. (a) Conventional hybrid-ring directional coupler. (b) Generalized hybrid-ring directional coupler.

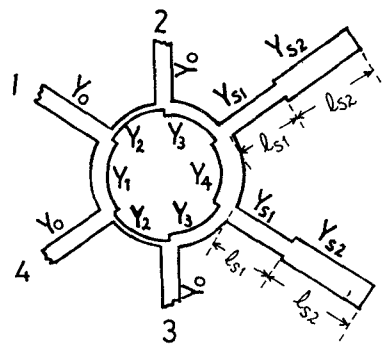

Fig 2 Generalized hybrid-ring with the assumed compensatng circuits attached to the hypothetical ports

M as follows:

$$M = \sum_{j=1}^{N}\left\{a_{j1}|S_{11}|^2 + a_{j2}|S_{22}|^2 + a_{j3}|S_{33}|^2 + a_{j4}\left(|S_{12}| - \frac{1}{\sqrt{2}}\right)^2 + a_{j5}\left(|S_{14}| - \frac{1}{\sqrt{2}}\right)^2 + a_{j6}\left(|S_{23}| - \frac{1}{\sqrt{2}}\right)^2\right\}_{f_j} \tag{3}$$

where N is the number of sampling points, f_j's are the sampled frequencies, and a_{ji}'s are the weighting coefficients for broad-band design.

Thus, the values of the parameters of Y_1 through Y_4, Y_{s1} and Y_{s2}, and l_{s1} and l_{s2} can be obtained numerically so as to minimize M and broaden the bandwidth widely as much as possible where the responses are within the extent of the given tolerance limits. In this case, the values of Y_s are determined uniquely since Y_{s1} always converges to zero no matter how the weighting coefficients a_{ji}'s take any values in the lossless case. On the other hand, the values of Y_1 through Y_4 computed by minimizing M are

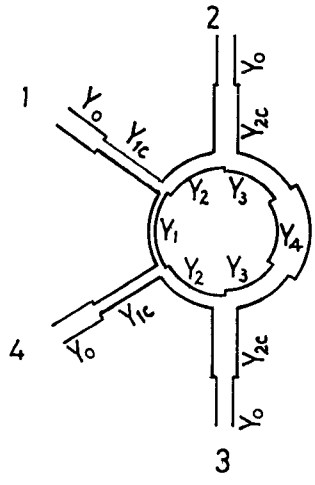

Fig. 3. Configuration of an improved hybrid ring.

not unique. They depend on the choice of a_{ji}'s and f_j's. Thus, the weighting coefficients a_{ji}'s and the sampling frequencies f_j's have great significance in computations of the optimum values. Hence, for the optimum values, we select the values of parameters which make the bandwidth widest within the extent of the tolerance limits for all responses by adjusting a_{ji}'s and f_j's.

Furthermore, it was proved that the bandwidth of the generalized hybrid-ring gets wider than the conventional hybrid-ring, and that excellent performance over bandwidth exceeding 50.6 percent can be obtained by the same method after adding quarter-wave transformers to the ports of the generalized hybrid-ring as shown in Fig. 3, without compensating circuits for the hypothetical ports.

III. Numerical Results

We took 2 or 4 sampling points of frequencies at appropriate intervals and proper weighting coefficients, and computed the optimum characteristic admittances Y_1 through Y_4 on the ring circumference, admittances Y_{s1} and Y_{s2}, and lengths l_{s1} and l_{s2} for the compensating stubs at the hypothetical ports by Powell's minimizing method [4]. We report, in Section IV, the numerically optimized results for the improved hybrid rings in comparison with the conventional hybrid ring.

First, the best condition of the hypothetical ports is found to be open-circuited since Y_{s1} always converges to zero in the lossless case, while the bandwidth above an octave could be obtained if negative $\partial Y_s/\partial f$ could be realized. Since a negative derivative of susceptance with respect to frequencies for a lossless circuit cannot be realized as is known from Foster's theorem, the open-circuited condition for the hypothetical ports is found to be the optimum terminating condition. Next, the optimum characteristic admittances Y_1 through Y_4 are obtained as shown in Table I, and thus, the bandwidth of the generalized hybrid ring gets wider, so it reaches up to 122.6 percent of the conventional rat race ring. The characteristics of the generalized 3-dB hybrid-ring shown in Table I are represented in Fig. 4(b) in terms of the couplings, reflection, and isolation, while the characteristics of the conventional rat race ring are represented in Fig. 4(a). Considering the simplification of the construction of the circuit, let Y_4 be equal to Y_3. Then the bandwidth obtained is almost the same as the generalized case of $Y_4 \neq Y_3$ as shown in T1-b and T1-c of Table I, while the frequency responses for the case of T1-c get very slightly worse than the case of T1-b in terms of the deviations of couplings.

In the case of the design method of the conventional hybrid-ring

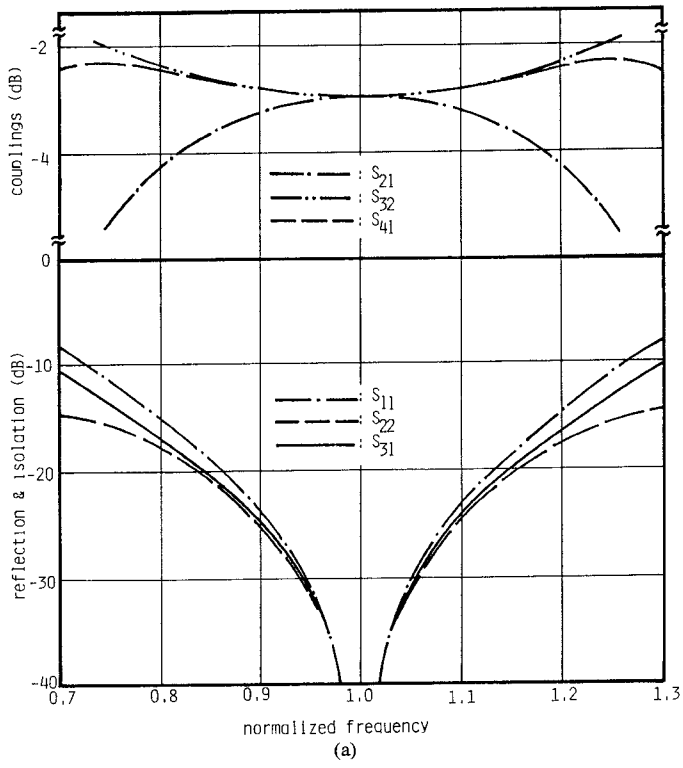

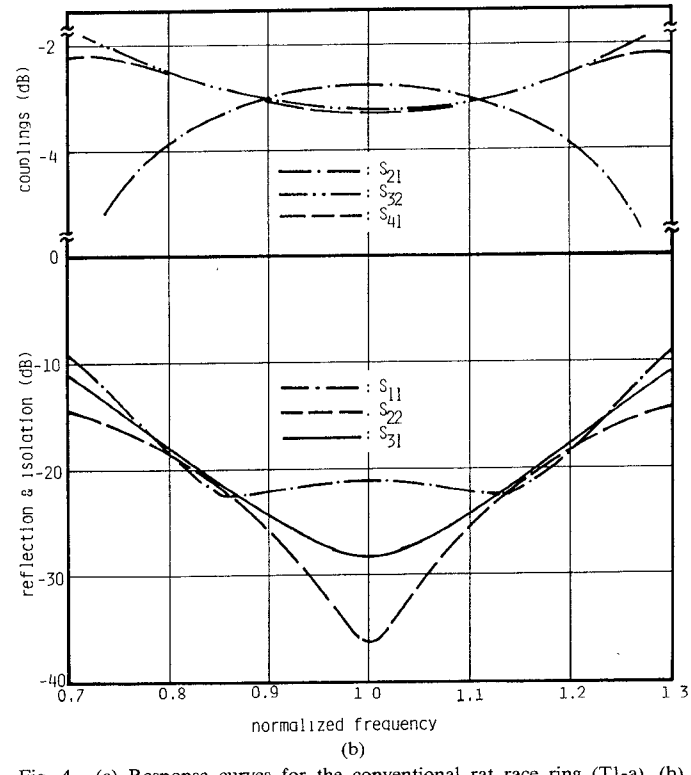

Fig. 4. (a) Response curves for the conventional rat race ring (T1-a). (b) Response curves for the generalized 3-dB hybrid ring (T1-b).

[2], [5], one can design a matched power divider with any desired power ratio by using the proper admittances Y_1 and Y_2 as putting $Y_1 = Y_3 = Y_4$ as the original. It can be observed that for equal power split, i.e., $S_{12}/S_{14} = 1$, and Y_1 and Y_2 are equal to $1/\sqrt{2}$ which is recognized as the admittance for the well-known 3-dB rat race ring. The bandwidth of the conventional rat race or hybrid-ring, however, does not exceed 27.6 percent, even though it operates perfectly at the center frequency. Therefore, the subs-

TABLE I
OPTIMUM VALUES OF THE PARAMETERS AND BANDWIDTH OF THE CONVENTIONAL RAT RACE AND THE GENERALIZED 3-DB HYBRID RING

	Y_1	Y_2	Y_3	Y_4	Bandwidth	Remarks
T1-a	0.70710	0.70710	0.70710	0.70710	27.56%	conventional rat race
T1-b	0.78186	0.76525	0.68114	0.69205	33.37%	generalized ($Y_3 \neq Y4$)
T1-c	0.78240	0.76488	0.66853		33.37%	generalized under $Y_3=Y_4$

* Y_1 through Y_4 are normalized admittances.

tance of the conventional design method for the hybrid-ring was not on broadening the bandwidth but only on dividing power with any desired ratio. Moreover, in the conventional rat race or hybrid-ring, the bandwidth under the given tolerance limits of all the responses is not to be broadened any more without dividing the three-quarter-wave equal-admittance section into unequal-admittance sections as the generalized hybrid-ring. Even though we add quarter-wave transformers to the original ports of the conventional rat race or hybrid-ring, as is often used for broadbanding, the bandwidth does not get wider at all. Here we will show an example. Fig. 5 shows the frequency responses of the conventional 3-dB hybrid-ring in Fig. 1(a) when optimized about Y_1 and Y_2 including the characteristic admittances of the quarter-wave transformers after adding quarter-wave transformers to the original ports for broadbanding without dividing the three-quarter-wave equal-admittance section into unequal-admittance sections. We can see from Fig. 5 that the bandwidth is not broadened compared to the original rat race or hybrid ring.

On the other hand, the bandwidth of one lambda ring (reverse-phase hybrid-ring) [5]–[7] may be increased to approximately an octave by substituting the coupled line quarter-wave section for the three-quarter-wave section of the conventional or original hybrid-ring (1.5 $-\lambda$ ring). This circuit would then make a ring equal to 1.0 wavelength in circumference. It is necessary to short-circuit the ends of the coupled line sections, which makes this difficult to construct and, therefore, limits its use to the lower frequencies where these short-circuits may be conveniently constructed. An additional broad-band magic tee concept was developed by Alford and Watts [8] and was further developed by Tatsuguchi [9]. These hybrids have not found wide acceptance because of their extreme difficulty of construction, although it has been the author's experience that at frequencies through *S*-band, their performance is excellent when carefully manufactured.

Since it is recognized from the above investigation that the best conditions of the hypothetical ports are open-circuited, we consider the generalized 3-dB hybrid-ring to which quarter-wave transformers are added, as shown in Fig. 3. In the same manner as the above, the optimum values of the characteristic admittances of Y_1 through Y_4, Y_{1c} and Y_{2c} are obtained as shown in Table II, where Y_1 and Y_4 are the optimum characteristic admittances on the circumference, Y_{1c} and Y_{2c} are the optimum admittances of the quarter-wave transformers. These optimized broad-band 3-dB hybrid rings which have the quarter-wave transformers added to the generalized hybrid ring without other compensating circuits are referred to as the *improved 3-dB hybrid-ring directional couplers* since they are extremely improved in comparison with the conventional rat race or hybrid ring. The parameters of Y_1 through Y_4, Y_{1c}, and Y_{2c} in the case of T2-a in Table II were optimized without any restrictions so that the bandwidth is 1.84 times as wide as the conventional rat race, extending to 50.67 percent, the frequency characteristics of which are shown in Fig. 6. For some applications, such as to microstrip

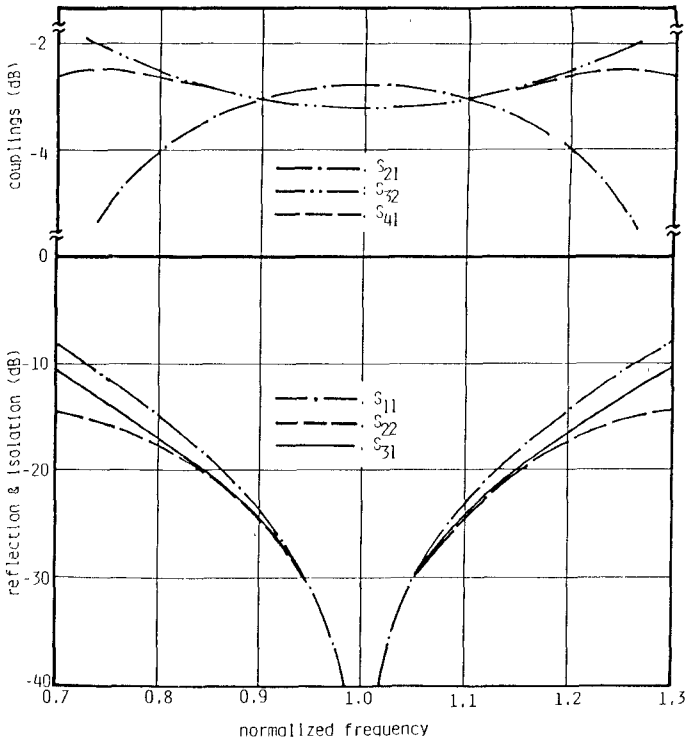

Fig. 5. Response curves for the conventional hybrid ring when optimized about Y_1 and Y_2 including quarter-wave transformers.

TABLE II
OPTIMUM VALUES OF THE PARAMETERS AND BANDWIDTH OF THE IMPROVED 3-DB HYBRID-RING DIRECTIONAL COUPLERS

	Y_1	Y_2	Y_3	Y_4	Y_{1c}	Y_{2c}	Bandwidth	Remarks
T2-a	0.88034	1.34850	3.57850	7.7350	1 05570	1.72860	50.67%	optimized
T2-b	0.88023	1.07190	1 82070	3.0	1.07160	1 34580	45.33%	optimized
T2-c	0.85517	1.07060	1.66050	2.5	1.05500	1.37250	44.44%	by
T2-d	0.86087	0.98403	1 36840	2.0	1.05890	1 24130	43.55%	specifying
T2-e	0.67781	0.82789	1 15230	1.5	0.93429	1.18500	39.11%	Y_4
T2-f	0.74460	1.01140	1.12800		0.99623	1.37580	36.44%	optimized under $Y_3=Y_4$

* Y_1 through Y_{2c} are normalized admittances.

line circuits, it is extremely difficult to fabricate, since the normalized characteristic admittance Y_4 above is as large as 7.735. Thus, it is desired to design a broad-band 3-dB hybrid ring with values of the admittances which may be fabricated easily. Hence, the parameters with appropriate values for all the admittances were obtained by optimization of (3) as the above after specifying the value of Y_4. When, for example, Y_4 was specified as 3, 2.5, 2, and 1.5, respectively, in normalized admittances, then the other parameters with the broadest bandwidth for each case within the tolerance limits of couplings, reflection, and isolations were obtained as shown in T2-b through T2-e of Table II. We can see from Table II that as Y_4 decreases, the bandwidth becomes narrower. Therefore, it can be optimally designed by specifying Y_4 as large as can be fabricated, not exceeding 7.735.

Considering the simplification of the construction of the circuits, let Y_4 be equal to Y_3 and the parameters of the improved 3-dB hybrid ring be optimized. Then, the relative bandwidth obtained is 36.44 percent, which is obviously compressed in comparison with the case of $Y_4 \neq Y_3$ on the three-quarter-wave section as shown in T2-f of Table II, even though its bandwidth is

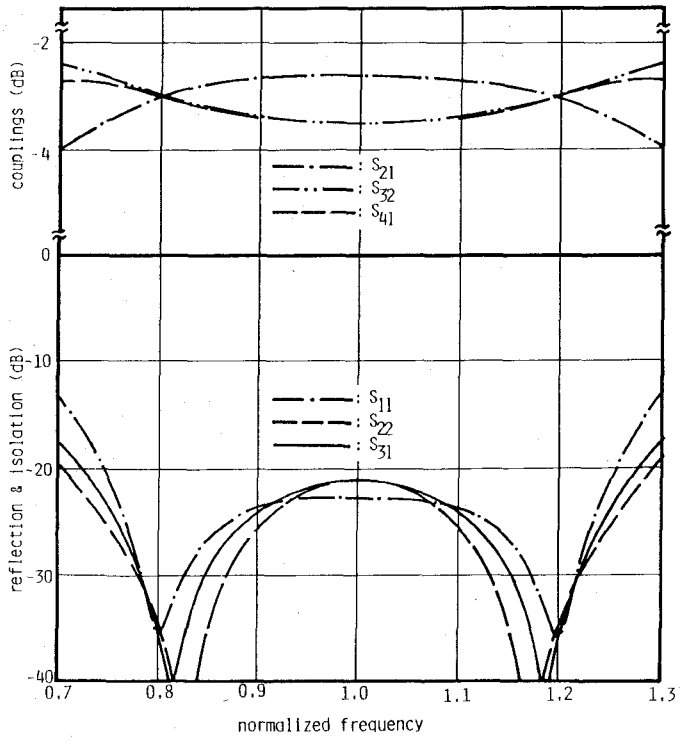

Fig. 6. Response curves for the improved 3-dB hybrid ring of T2-a.

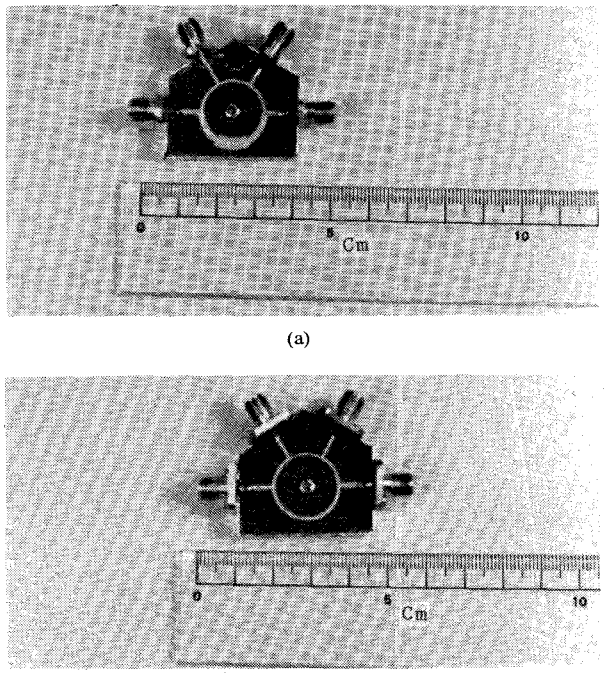

Fig. 7. (a) Photograph of the improved hybrid ring (T2-b). (b) Photograph of the improved hybrid ring (T2-f).

broader than the conventional rat race or hybrid-ring. Thus, it was clearly proven that replacing the three-quarter-wave section of the conventional hybrid ring with Y_3 of the two quarter-wave sections and Y_4 of the one quarter-wave section by applying the concept of hypothetical port is valid and effective for the broad-band design of a circuit like the hybrid-ring directional coupler. The broad-band design method previously described is also applicable to a hybrid-ring directional coupler with any degree of coupling.

IV. Experimental Results

To confirm that the improved 3-dB hybrid-ring directional couplers proposed here have excellent performance, we have fabricated the circuits of T2-b and T2-f in Table II on microstrip line and tested their frequency characteristics. The effective dielectric constant, the wavelength, and the line impedance in the microstrip can be calculated by [10]

$$\epsilon_{\text{eff}} = \frac{\epsilon_r + 1}{2} + \frac{\epsilon_r - 1}{2}\left(1 + 10\frac{h}{w}\right)^{-1/2}$$
$$\lambda_g = \lambda_0/\sqrt{\epsilon_{\text{eff}}}$$
$$z = z_0/\sqrt{\epsilon_{\text{eff}}} \tag{4}$$

where

$$z_0 = \frac{120\pi(\Omega)}{W/h + 2.42 - 0.44h/W + (1 - h/W)^6} \qquad \text{for } W/h > 1.$$

W is the width of the line, and h is the thickness of the dielectric substrate. The calculated values for constructing the improved 3-dB hybrid rings of T2-b and T2-f at the center frequency of 6 GHz by (4) are tabulated in Table III. The circuits used for experiments are shown in Fig. 7(a) and (b). Because of the variation in effective dielectric constant in microstrip, the lengths of the quarter-wave sections on the ring circumference should be different from one another. However, in the experiments we constructed the networks conveniently and easily by using the mean value of the wavelengths on the circumference, i.e., neglecting the differences of the wavelengths due to the differences of the line impedances. The dielectric substrate used here has the dielectric constant ϵ_r of 2.6 and the thickness h of 254 μm.

TABLE III
Values for the Construction of the Improved 3-dB Hybrid Ring Directional Couplers Used in Experiments

	Y	Line Impedance	ϵ_{eff}	λ_g (mm)	W/h	W (mm)
T2-b	Y_1	56.80 (Ω)	2.144	34.14	2.275	0.580
	Y_2	46.65	2.189	33.80	3.090	0.788
	Y_3	27.46	2.289	32.98	6.347	1.618
	Y_4	16.67	2.387	32.36	11.674	2.977
	Y_{1c}	46.66	2.189	33.80	3.088	0.788
	Y_{2c}	37.15	2.237	33.43	4.266	1.088
T2-f	Y_1	67.15	2.105	34.46	1.703	0.434
	Y_2	49.44	2.176	33.90	2.832	0.722
	$Y_3=Y_4$	44.33	2.200	33.71	3.329	0.849
	Y_{1c}	50.19	2.172	33.92	2.767	0.706
	Y_{2c}	36.34	2.242	33.39	4.395	1.121

* the relative dielectric constant ϵ_r = 2.60.
the thickness of substrate h = 254 μm
the design center frequency f_o = 6GHz

Figs. 8(b) and 9(b) show the measured frequency characteristics obtained from the experimental improved 3-dB hybrid-ring directional couplers of T2-b and T2-f constructed approximately and easily by the previous manner, while the theoretical responses are shown in Figs. 8(a) and 9(a), respectively. Here, it was confirmed that the performance of the improved 3-dB hybrid-ring directional coupler is excellent, and, hence, the bandwidth of these circuits were 46.2 percent and 34.6 percent for

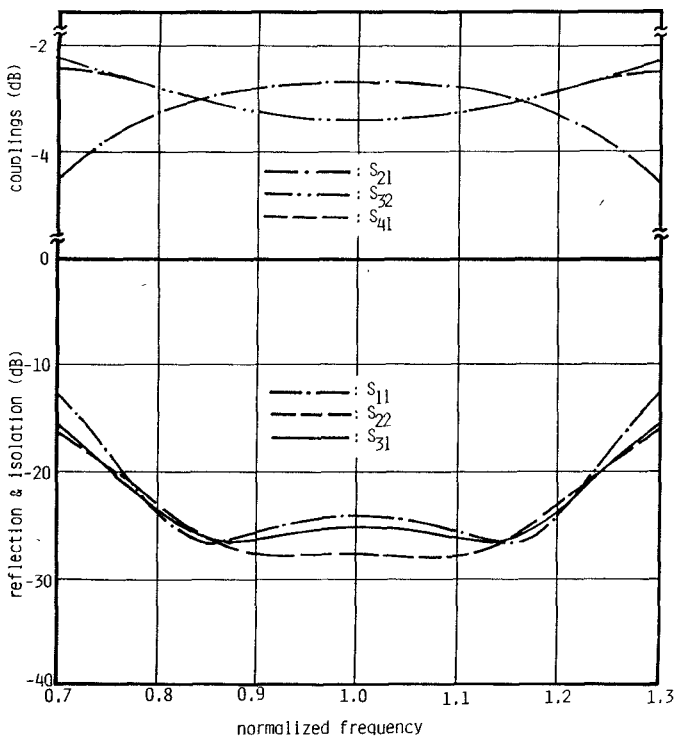

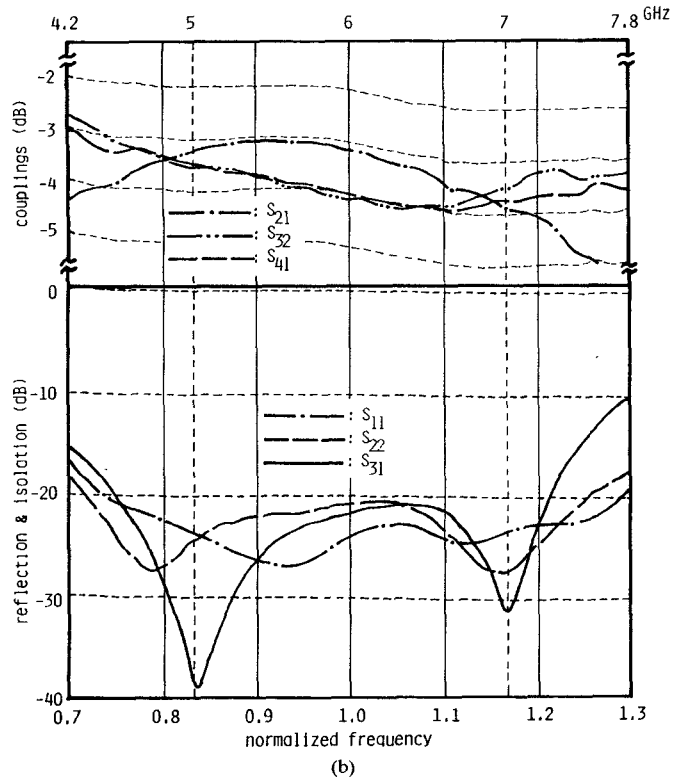

Fig. 8. (a) Theoretical frequency characteristics of the improved hybrid ring (T2-b). (b) Measured frequency characteristics of the improved hybrid ring (T2-b).

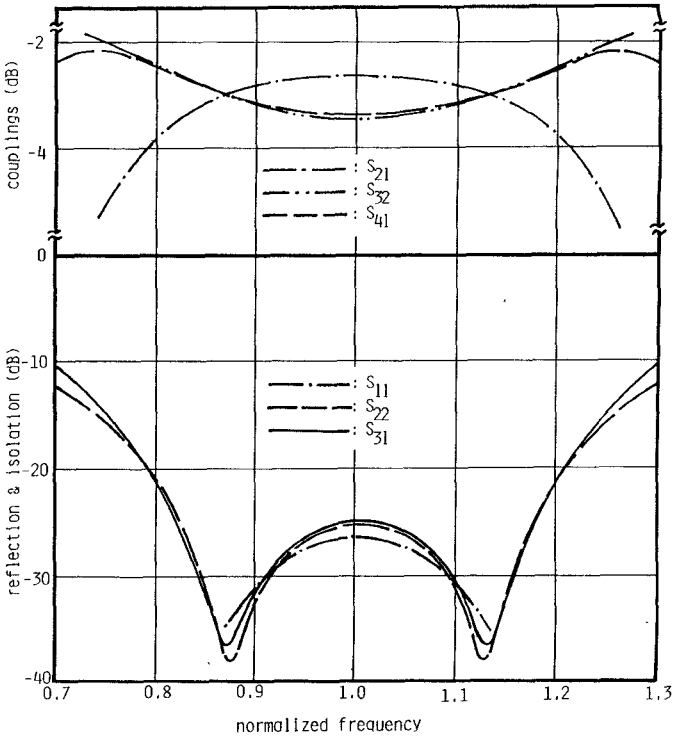

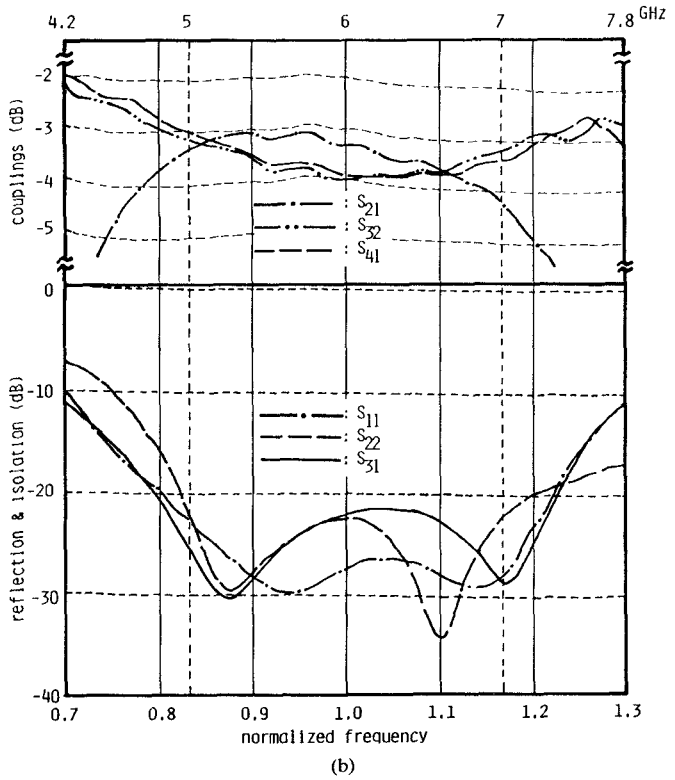

Fig. 9. (a) Theoretical frequency characteristics of the improved hybrid ring (T2-f). (b) Measured frequency characteristics of the improved hybrid ring (T2-f).

T2-b and T2-f, while the designed bandwidths are 45.3 percent and 36.4 percent, respectively. The frequency characteristics agree reasonably well with the designed ones in spite of neglecting the wavelength differences at the ring sections. Thus, the improved hybrid-ring directional couplers with broadbands proposed in this paper can be fabricated very easily.

On the other hand, the levels of equal splits fell down to about 3.5 dB due to losses. Especially in the case of T2-f, since the loss for S_{21} is relatively high in the high frequency band, the useful bandwidth of the device T2-f is compressed to 34.6 percent, though the designed one is 36.9 percent in terms of 20-dB return loss and isolation. Therefore, it is expected that the performance

of the improved 3-dB hybrid-ring directional coupler would be better when carefully and elaborately manufactured.

V. Conclusion

A broad-band design theory of the improved 3-dB hybrid-ring directional couplers by CAD was demonstrated, where the concept of a hypothetical port was adopted. Also, the characteristics of the improved 3-dB hybrid ring are compared with those of the conventional rat race and hybrid ring. It was clearly shown that the bandwidth is broadened considerably by dividing the three-quarter-wave equal-admittance section of the conventional hybrid-ring into unequal-admittance sections with proper values, while the symmetry of the circuit is maintained. Hence, the improved hybrid-ring directional coupler can be constructed very easily and its bandwidth reaches up to approximately 50.7 percent. The experiments for two cases as examples were carried out, the results of which agreed well with the numerically designed ones, and, hence, the validity of the broad-band design method was confirmed.

Acknowledgment

The authors would like to express their thanks to Dr. K. Araki who gave them valuable advice.

References

[1] H. Kurebayashi, "Design method of the compact microstrip circulator with the junction loaded with impedance," Tech Rep. IECE Japan, MW76-85, pp. 71–78, Oct. 1976
[2] C Y Pon, "Hybrid-ring directional coupler for arbitrary power division," *IRE Trans. Microwave Theory Tech.*, vol. MTT-9, pp. 529–535, Nov. 1961.
[3] J. Reed and G J Wheeler, "A Method of analysis of symmetrical four-port network," *IRE Trans. Microwave Theory Tech.*, vol. MTT-4, pp. 246–252, Oct. 1956.
[4] M. J D. Powell, "A Method for minimizing a sum of squares of nonlinear functions without calculating derivatives," *Computer J.*, vol. 7, pp. 303–307, 1965.
[5] H Howe, Jr., *Stripline Circuit Design* New York: Artech House, 1979, pp 85–94
[6] M. Aikawa, "Wide-band stripline reverse-phase hybrid-ring in GHz band," *Trans IECE*, Japan, vol. 58-B, no. 10, pp. 521–528, Oct 1975.
[7] S. March, "A wideband stripline hybrid ring," *IEEE Trans. Microwave Theory Tech.*, vol. MTT-16, no. 6, p. 361, June 1968.
[8] A. Alford and C. B. Watts, "A wide-band coaxial hybrid," in *IRE Convent. Rec.*, Part 1, 1956, pp. 176–179.
[9] I. Tatsuguchi, "UHF-strip transmission line hybrid junction," *IEEE Trans. Microwave Theory Tech.*, vol. MTT-9, no. 1, pp. 3–6, Jan. 1961.
[10] M. V. Schneider, "Microstrip lines for microwave integrated circuits," *Bell Syst. Tech. J.*, pp. 1421–1445, May–June 1969.

New View on an Anisotropic Medium in a Moving Line Charge Problem

MASANORI KOBAYASHI, MEMBER, IEEE

***Abstract*—The electromagnetic field solution of the problem, in which the line charges move uniformly parallel or perpendicular to the interface of two different anisotropic media, is obtained by the method of moving images. The results are shown by representing the moving image line charges for such a problem. A new view on an anisotropic medium in such a problem is discussed by defining the equivalent metric factor and the equivalent normalized metric factor. The minimum principle shown in this short paper states that the electric flux emitted from the moving line charge chooses a trajectory that minimizes the equivalent effective length.**

Manuscript received March 9, 1982; revised May 4, 1982.
The author is with the Department of Electrical Engineering, Ibaraki University, 4-12-1 Nakanausawa-Machi, Hitachi, Ibaraki, Japan

I. Introduction

The radiation produced by a uniformly moving point charge has been experimentally discovered by Cerenkov [6] and theoretically investigated by Frank and Tamm [7]. Ginzburg and Frank [8] have shown that a point charge moving uniformly across the interface of two media with different dielectric constants emits a unique radiation, called transition radiation. These radiations have later markedly been investigated by many workers [1]–[5], [9]–[17] (good bibliographies are given in [15] and [20]). The Cerenkov counter (for example, see [4]) and the microwave generator (for example, see [1], [5]) have been considered as the application. On the other hand, the problem of radiation from a source embedded in a moving medium as the inverse problem of the former has been investigated (for example, see [18]–[20], good bibliographies are given in [20]).

From the interests for the boundary value problem in the relativistic electrodynamics, this short paper treats the fields produced by moving charges. The fields produced by charges moving uniformly in two isotropic media have been determined, by the method of moving images, by Beck [9] for the motion perpendicular to the interface and by Sitenko and Tkalich [13] for the motion parallel to the interface.

This short paper derives the solution of electromagnetic fields by the line charges uniformly moving parallel or perpendicular to the interface of two different anisotropic media. This problem may be attacked by the method of moving images for a case that the velocities of all moving line charges are less than the phase velocities of light in those media. Then, the equivalent metric factor and the equivalent normalized metric factor of an anisotropic medium are defined by extending the metric factor and the normalized metric factor in the case of the static problem [21]. The minimum principle of equivalent effective path length for such electric flux is expressed in the form of integration by using the equivalent normalized metric factor.

II. Fields by a Moving Line Charge in a Single Anisotropic Medium

Consider the problem that the line charge λ_0 infinitely extended parallel to the x axis moves uniformly in the positive z-direction with velocity v in a single medium of the following permittivity tensor $\bar{\epsilon}$ and permeability μ:

$$\bar{\epsilon} = \begin{pmatrix} \epsilon_x^* & 0 & 0 \\ 0 & \epsilon_y^* & 0 \\ 0 & 0 & \epsilon_z^* \end{pmatrix} \epsilon_0 \tag{1}$$

$$\mu = \mu^* \mu_0 \tag{2}$$

where ϵ_x^*, ϵ_y^*, and ϵ_z^* are the relative dielectric constants, μ^* the relative permeability, and ϵ_0 and μ_0 the permittivity and the permeability of vacuum, respectively.

The electromagnetic field is determined by Maxwell's equations for the given line charge density and current

$$\rho_0 = \lambda_0 \delta(y)\delta(z - vt) \tag{3}$$

$$j = \rho v \hat{z} \tag{4}$$

0018-9480/82/1100-2046$00.75 ©1982 IEEE